The overdoped colossal magnetoresistive manganites

2007 J. Phys.: Condens. Matter 19 125218

(http://iopscience.iop.org/0953-8984/19/12/125218)

IOP PUBLISHING JOURNAL OF PHYSICS: CONDENSED MATTER

J. Phys.: Condens. Matter **19** (2007) 125218 (21pp) doi:10.1088/0953-8984/19/12/125218

The overdoped colossal magnetoresistive manganites

A Taraphder

Department of Physics and Meteorology and Centre for Theoretical Studies, Indian Institute of Technology, Kharagpur 721302, India

E-mail: arghya@phy.iitkgp.ernet.in and arghya@cts.iitkgp.ernet.in

Received 24 August 2006
Published 6 March 2007
Online at stacks.iop.org/JPhysCM/19/125218

Abstract

The rich physics in the overdoped regime in colossal magnetoresistive manganites is discussed in detail. Apart from having a large magnetoresistance like its underdoped counterpart, the overdoped regime offers a rich variety of phenomena including magnetic, charge and orbital order at low temperatures. The antiferromagnetic metallic state with anisotropic carrier transport, low-dimensional magnetic states and a broad spectrum of excitations is discussed. It is argued that the physics in the overdoped regime is primarily governed by the coupling of orbitals and spins. The Jahn–Teller effect, considered to be crucial for the understanding of underdoped manganites, does not play a major role in the overdoped region. The inadequacy of the limit of infinite Hund's coupling in describing the manganites, and the importance of Coulomb correlations, are borne out in several examples described. Bilayer manganites, owing to their layered structures, are shown to have an effectively stronger coupling with the underlying structural distortions. The charge ordering close to $x = 0.5$ and the effect of changing bandwidth are discussed. The effect of disorder and the possibility of having an inhomogeneous mixture of competing states are also outlined.

(Some figures in this article are in colour only in the electronic version)

1. Introduction

In the last 20 years the field of correlated electrons has seen some major developments. Beginning with the discovery of high temperature superconductivity followed a decade later by the observation of colossal magnetoresistance (CMR) in manganites, there has been tremendous progress in the understanding of correlated systems, though the initial euphoria about the technological fallout has given way to a somewhat less dramatic but steady growth in their applications. There is also a very significant development in the experimental techniques, made necessary by the complexity of these systems, that has revealed fascinating mechanisms and new frontiers during this period.

The manganites with generic formula $R_{1-x}A_xMnO_3$, where R and A stand for trivalent rare-earth (e.g., La, Nd, Pr, Sm) and divalent alkaline-earth ions (Ca, Sr, Ba, Pb etc) respectively, were studied in the 1950s by a number of groups [1, 2, 15, 3] and their magnetic, orbital and transport properties inspired several experimental and theoretical investigations. These are the three dimensional, $n = \infty$ member of a chemical series of layered perovskites called the Ruddlesden–Popper (RP) series, with formula unit $(R, A)_{n+1}Mn_nO_{3n+1}$ (R = rare earth, A = alkaline earth). The connection between their transport properties and the underlying ferromagnetic ground state was established by van Santen [1], and a simple and elegant explanation was put forward by Zener [10], introducing the concept of double exchange (DE). When 'colossal' negative magnetoresistance was reported [8, 9] in the early 1990s in $La_{1-x}Ca_xMnO_3$ around the same temperature where a ferromagnetic transition takes place, new experimental and theoretical developments, already in place owing to ten years of intense research on high T_c, were brought to bear upon these systems with immediate and spectacular effect (for general reviews see [5–7, 11, 25] and references therein).

The initial thrust of research in manganites was in the doping region of $0 < x < 0.5$ where the CMR and the nearly concomitant ferromagnetic (FM) order is observed. It was realized within a few years that the region $0.5 \leqslant x \leqslant 1$ too is endowed with very large MR, particularly in the larger bandwidth materials like $Nd_{1-x}Sr_xMnO_3$ [18, 19] and $Pr_{1-x}Sr_xMnO_3$ [21, 22, 29], and this region is also replete with fascinating physics. The charge, spin, orbital and lattice degrees of freedom of the manganites are all coupled strongly in the underdoped regime and the same is true for the overdoped region as well [23–25]. It is this coupling between all these degrees that leads to stimulating physics [26].

It was noticed that there is no symmetry between the phase diagram of the region $x > 0.5$, the overdoped regime[1], and the phase diagram in the $x < 0.5$ region and the underlying physics of the overdoped region is different from its $x < 0.5$ counterpart. The DE model, in which the itinerant electrons are coupled to the localized spins at the manganese ions through Hund's exchange, predicts qualitatively similar physics above and below $x = 0.5$. The lack of symmetry between $x < 0.5$ and $x > 0.5$, manifested most strikingly in the magnetic phase diagram of the CMR manganites, therefore, calls for a considerable revision in the way one looks at the overdoped region. In response to these and other observations discussed below, theoretical approaches have now been developed for the overdoped region [37, 39, 40, 74]. These ideas were then successfully applied to the overdoped bilayer manganites [75, 76] (the $n = 2$ member of the RP series) when their phase diagram and physical properties became available later on. It is difficult to accommodate all the developments in this area, both experimental and theoretical, in a terse review. In what follows, I will try to give an account of the overdoped manganites from a general and broad perspective.

2. Physical properties

Several careful studies [19, 28, 31, 35] have now established that the systems $Nd_{1-x}Sr_xMnO_3$, $Pr_{1-x}Sr_xMnO_3$ and $La_{1-x}Sr_xMnO_3$ are antiferromagnetically ordered beyond $x = 0.5$, while one observes either a metallic ferromagnetic state or a charge-ordered (CO) state with staggered charge ordering [30] in the approximate region $0.25 < x < \frac{1}{2}$. The antiferromagnetic (AFM) order in the overdoped region, shown in figure 1, varies with x from A-type (a planar spin order, FM planes coupled antiferromagnetically across) to C-type (AFM planes coupled

[1] If one uses the $x = 1$ composition (e.g., $CaMnO_3$) as the parent material, instead of the $x = 0$ composition (such as $LaMnO_3$), then the doping of trivalent atoms for the divalent ones (La for Ca, for example) involves adding electrons in the e_g band. This regime is, therefore, also called the *electron-doped regime* in the literature.

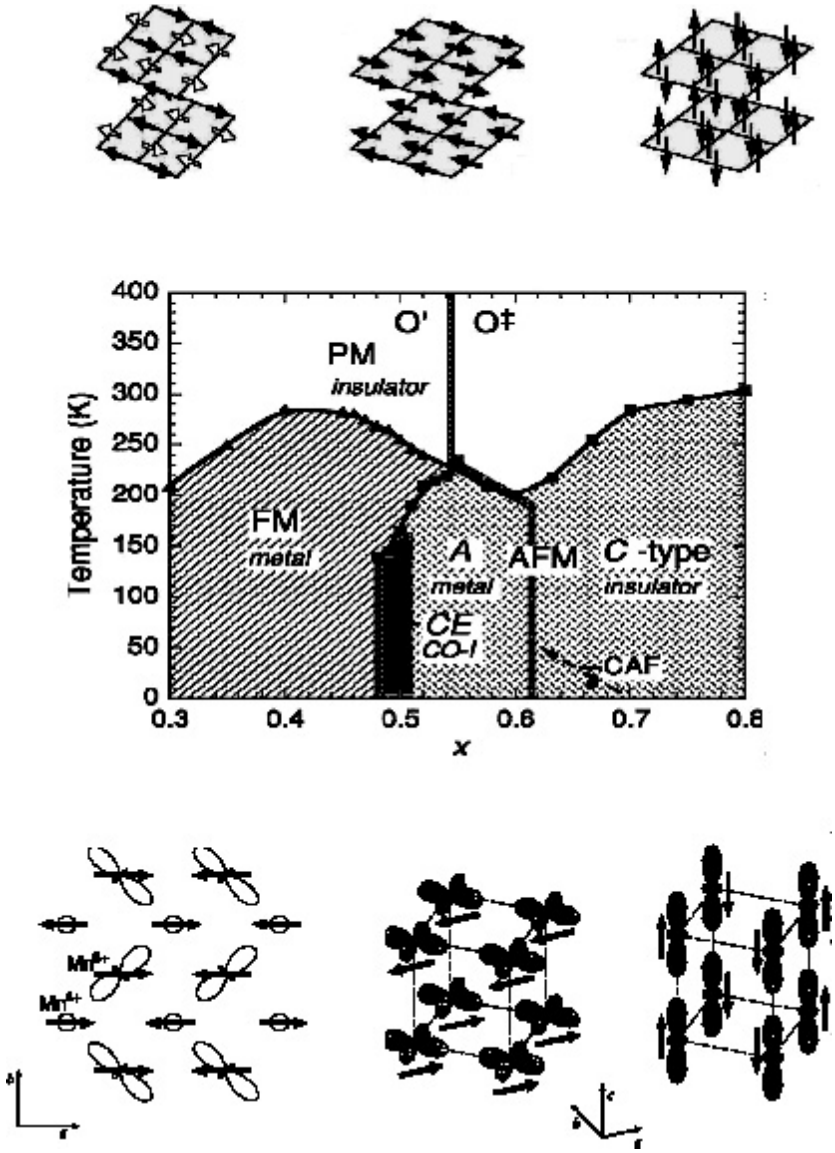

Figure 1. Magnetic phase diagram of $Nd_{1-x}Sr_xMnO_3$ (reprinted with permission from Kajimoto *et al* [35], copyright (1999) by the American Physical Society). PM and CAF stand for paramagnetic and canted AFM. CO-I designates charge ordered insulator. Close to $x = 1$, a G-type AF phase appears. The upper and lower panels describe the spin and orbital order respectively (from left to right) in the CE-phase, A-phase and C-phase.

ferromagnetically) to the usual 3D staggered spin order close to $x = 1$, referred to as the G-type order. The stability of these regions also depends on the conduction bandwidth of the material. For example $La_{1-x}Sr_xMnO_3$, the manganite with the largest bandwidth, shows an A-type AFM ground state in the range $0.52 < x < 0.58$. It also shows a sliver of FM phase [28] immediately above $x = 0.5$. In $Nd_{1-x}Sr_xMnO_3$, a moderate bandwidth system [19, 35], the A-type spin structure appears at $x = 0.5$ and is stable up to $x = 0.62$, while in $Pr_{1-x}Sr_xMnO_3$ [21, 27] this region extends from $x = 0.48$ to 0.60. In all these cases, the one dimensional C-type phase

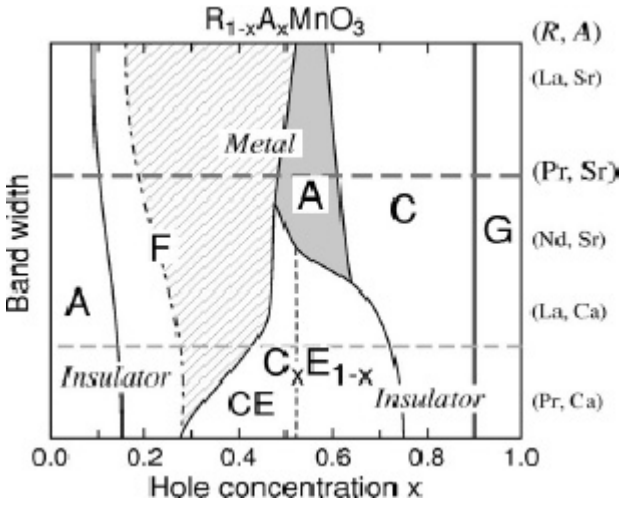

Figure 2. Phase diagram (schematic) showing the nature of magnetic ground states with changing band structure (reprinted with permission from Kajimoto *et al* [29], copyright (2002) by the American Physical Society). C_xE_{1-x} refers to incommensurate charge/orbital order.

abuts the two dimensional A-type order as x increases, giving way to the 3D G-type order at higher x. Kajimoto *et al* [29] have combined the phase diagrams of various manganites of varying bandwidths and this is shown schematically in figure 2. Note that the narrow bandwidth compounds, $Pr_{1-x}Ca_xMnO_3$, $La_{1-x}Ca_xMnO_3$ etc, exhibit a region of CE-type insulating charge-ordered (CO) state around $x = 0.5$ while $Nd_{1-x}Sr_xMnO_3$ shows the planar A-type antiferromagnetic order. As the bandwidth increases in compounds like $Pr_{1-x}Sr_xMnO_3$ and $La_{1-x}Sr_xMnO_3$, a small strip of FM metallic phase appears at $x = 0.5$ [28, 29] followed by the A-type AFM order. The wider bandwidth manganites show, in general, the following sequence of spin/charge order upon hole doping (for the entire range $0 \leqslant x \leqslant 1$): insulating A-type AFM $\rightarrow$ metallic FM $\rightarrow$ metallic A-type AFM $\rightarrow$ insulating C-type AFM and finally an insulating G-type AFM state. Clearly, one of the most striking features is the absence of CE-type spin/charge order and the presence of a metallic A-type AFM state in the moderate to large bandwidth magnitudes. The lower-bandwidth systems, on the other hand, show CE-type order in this commensurate doping region.

There has been a large number of reports of charge ordering and inhomogeneous states [18, 21, 45, 47, 48, 57, 71] in the region $x \simeq 0.5$. These states are quite abundant in the low bandwidth materials. In $(Nd_{1-y}Sm_y)_{0.5}Sr_{0.5}MnO_3$, the bandwidth has been systematically controlled [20] using both chemical substitution (Sm for Nd) and hydrostatic pressure to show the evolution of the charge order and the consequent metal–insulator transition. There are indications of stripe type charge order [29] in the neutron scattering of the half-doped $Pr_{1-x}Sr_xMnO_3$ ($x = 0.5$) in its A-phase region. The inhomogeneous states result from the competing ground states [11, 49, 61] (charge ordered/AFM and FM primarily) that lead to first order phase transitions with a discontinuity in the density as the chemical potential is varied. Such transitions are known to lead to phase separation in the canonical ensemble [46, 49, 50, 52–56, 74]. The charge ordered states are often very 'soft': they 'melt' into an FM metallic state on application of only a few Tesla magnetic field [21, 25]. Such macroscopic phase separations are not stable against long range Coulomb interactions and tend to break up into microscopic inhomogeneities [49, 53, 55].

The transport properties in this region follow the anisotropy of the magnetic order. The A-type order facilitates charge transport in the FM planes while the coherent transport of charges across the antiferromagnetically coupled planes is drastically reduced. In the C-type phase, similarly, the charge transport is coherent along the line of FM ordered spins in the c-direction and incoherent in the ab-plane. Both the A-type and the C-type phases are also orbitally ordered. The orbital order reverses across the A–C phase boundary, from a $d_{x^2-y^2}$ type orbital order in the A phase to a $d_{3z^2-r^2}$ type order in the C phase. There is also the observation, as in the underdoped region, of the 'melting' of the orbital order by a magnetic field [43] in $Nd_{1-x}Sr_xMnO_3$ at $x = 0.55$. What is remarkable is that the A-type spin order disappears and an FM metallic state appears as the orbital order is destroyed [43], lending strong support to the notion that it is the orbital order that pre-empts [42, 44, 74] the magnetic order in this regime. Zimmermann *et al* [45] observe from a resonant x-ray scattering experiment in $Pr_{1-x}Ca_xMnO_3$ at $x = 0.5$ that the charge and orbital order are linearly coupled and they form at a common temperature $T_{CO} \sim 245$ K. They also note that the CO/OO enhances AF fluctuations and finally leads to the AF transition at $T_N \sim 170$ K. The CO correlation lengths are found to be longer than the OO correlation length, though they order together. It is only natural, therefore, that with x increasing, as the CO is destroyed, the orbital order (which changes from CE type to a planar $d_{x^2-y^2}$ type) in the A-phase facilitates the AF magnetic order. Much of the evidence for the magnetic and orbital order comes from neutron scattering, transport and structural investigations. Some of these experimental results are reviewed in the following.

2.1. The ordered states

A large number of careful studies have been made to analyse the magnetic and orbital order in the overdoped region of manganites. Investigations with neutron scattering and resonant x-ray scattering have provided valuable information about the ordered states. Structural and transport data have been quite useful in corroborating the conclusions drawn from the neutron and x-ray scattering experiments.

One of the major observations in the region $x > 0.5$ was the antiferromagnetic metallic phase (the A phase) with a planar ferromagnetic order [28, 31] as mentioned already. Both $Nd_{1-x}Sr_xMnO_3$ and $Pr_{1-x}Sr_xMnO_3$ show an insulating AF order below $T_N \sim 150$ K at $x = 0.5$, but the resistivity of $Pr_{0.5}Sr_{0.5}MnO_3$ below T_N is $\sim 2 \times 10^{-2}$ Ω cm, nearly four orders of magnitude lower than the resistivity of $Nd_{0.5}Sr_{0.5}MnO_3$. This difference is attributed to the presence of a charge order in $Nd_{0.5}Sr_{0.5}MnO_3$. It was also found that at $x = 0.55$, $Nd_{1-x}Sr_xMnO_3$ no longer has this CE-type insulating state below (a higher) $T_N \sim 220$ K and its resistivity remains quite low ($\sim 10^{-3}$ Ω cm). Neutron diffraction studies [28, 31, 35] indicated that in this A-type AF state the spins are FM ordered in the ab-plane and antiparallel across. The insulating AF state of $Pr_{0.5}Sr_{0.5}MnO_3$ shows no indication of charge/orbital ordering, thereby ruling out the CE phase. Indeed the transport measurement showed a large anisotropy in the AFM state of $Nd_{1-x}Sr_xMnO_3$ at $x = 0.55$ [19]: ρ_{ab} is nearly four orders of magnitude lower than ρ_c at 35 mK. There is also a large field dependence of the resistivity (in both ρ_c and ρ_{ab}, though the effect is more dramatic in ρ_c [19]). The MR is negative and the change in ρ_c could be as high as 90% in 8 T field at low temperatures.

Neutron diffraction data on $Nd_{1-x}Sr_xMnO_3$ are quite representative in revealing the general trends observed in the overdoped manganites as a function of doping as shown in figure 3. Except for the small bandwidth systems like $Pr_{1-x}Ca_xMnO_3$, most manganites follow this general trend. As x increases from $x = 0.5$, there is a systematic transformation of the crystalline structure along with the magnetic order. The MnO_6 octahedra are apically compressed in both the CE-type phase at $x = 0.5$ and the A-type phase just beyond. The

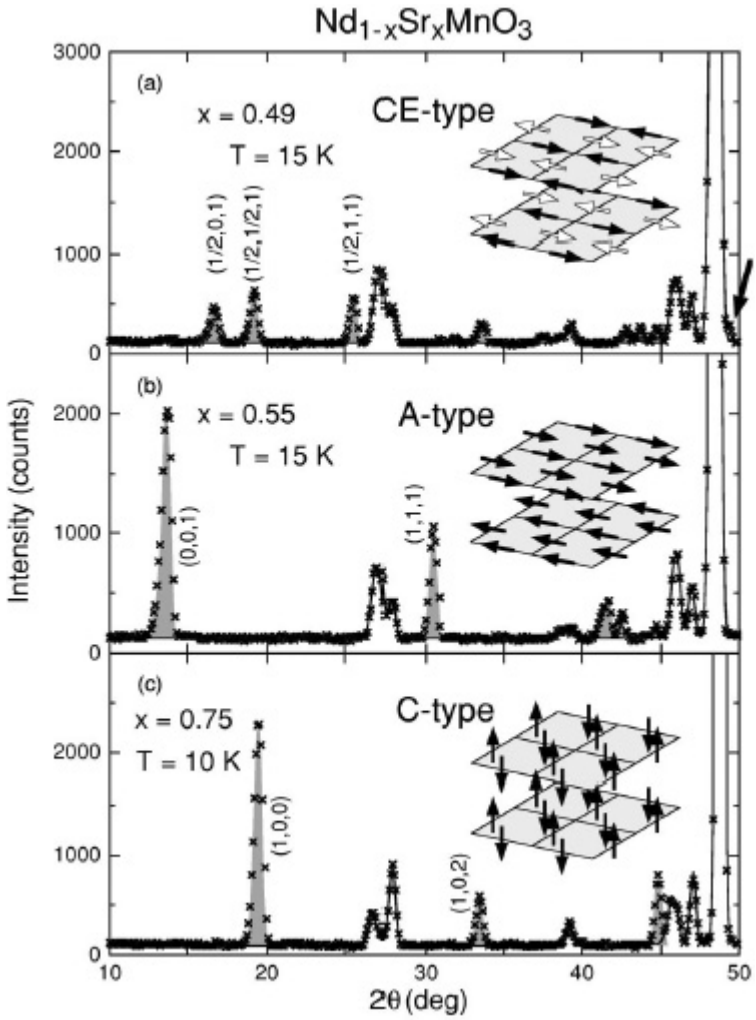

Figure 3. Powder diffraction intensity (low angle) at three different values of doping in $Nd_{1-x}Sr_xMnO_3$. The corresponding phases are shown in the insets with their respective spin arrangements (reprinted with permission from Kajimoto *et al* [35], copyright (1999) by the American Physical Society).

compression is correlated with the alternate $d_{3x^2-r^2}/d_{3y^2-r^2}$ order in the CE phase and the planar $d_{x^2-y^2}$ order in the A phase. In the C-type phase that appears beyond A type, the octahedra are elongated in the apical direction owing to rod-like $d_{3z^2-r^2}$ orbital order.

The carrier transport and magnetic/orbital order are related intimately in the low dimensional magnetic A and C phases. In figure 4 the magnetization, lattice parameters and resistivity of $Nd_{1-x}Sr_xMnO_3$ ($x = 0.55$) are shown following Kuwahara *et al* [19]. The magnetic moment is quenched below $T_N \simeq 220$ K while the increase of μ_B above T_N is due to the building up of FM correlations. The magnetization curve below T_N shows macroscopic anisotropy; the parallel magnetization along the [110] direction is slightly smaller than the perpendicular [001] magnetization. This evidently indicates a layered AF structure (the A type).

The magnetic and orbital orders are also coupled to the structural changes. Owing to the buckling of the MnO_6 octahedra the unit cell deviates from a perfect cubic structure and

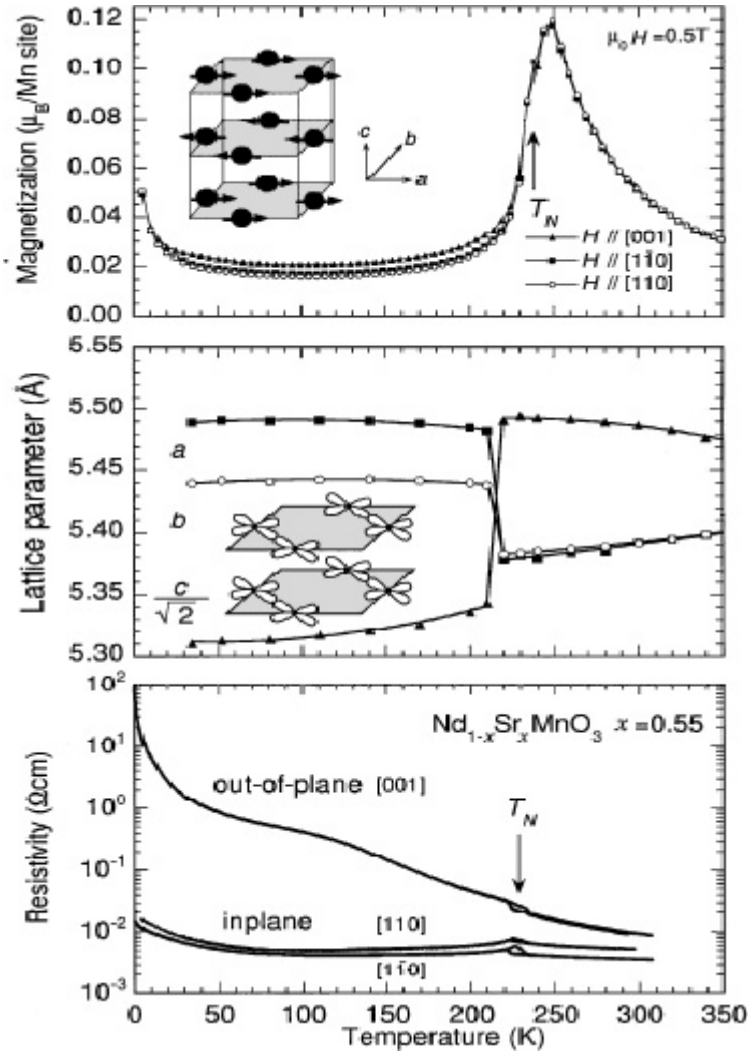

Figure 4. The three panels show temperature dependence of magnetization, lattice parameters and resistivity for a single crystal $Nd_{1-x}Sr_xMnO_3$ sample (reprinted with permission from Kuwahara *et al* [19], copyright (1999) by the American Physical Society). Note the rise of magnetization followed by the sharp drop as T_N approaches and the slight anisotropy due to layered magnetic structure (A phase). The magnetic and orbital orders are shown as insets in the top two panels.

becomes orthorhombic with dimensions $\sim\sqrt{2} \times \sqrt{2} \times 2$ of the cubic unit cell. Below T_N the pseudotetragonal $O^{\ddagger}$ phase with $a \simeq b < \frac{c}{\sqrt{2}}$ changes to orthorhombic O′ with lattice parameters $\frac{c}{\sqrt{2}} < b < a$. In figure 1 the separation between these two regions is shown. In the range $0.55 \leqslant x \leqslant 0.60$ the structural transition coincides with T_N. At the boundary between A and C phases, it is coincident with the A–C transition. This structural transition is illustrated in the middle panel of figure 4. The transformation to O′ is associated with the elongation in the ab-plane and compression in the c-direction. This is in accord with the $d_{x^2-y^2}$ orbital order in the A phase. The AF phase in undoped $LaMnO_3$ is also orbitally ordered, but the orbital order is staggered ($d_{3x^2-r^2}/d_{3y^2-r^2}$). The transition is first order (slight hysteresis noticed at T_N in the

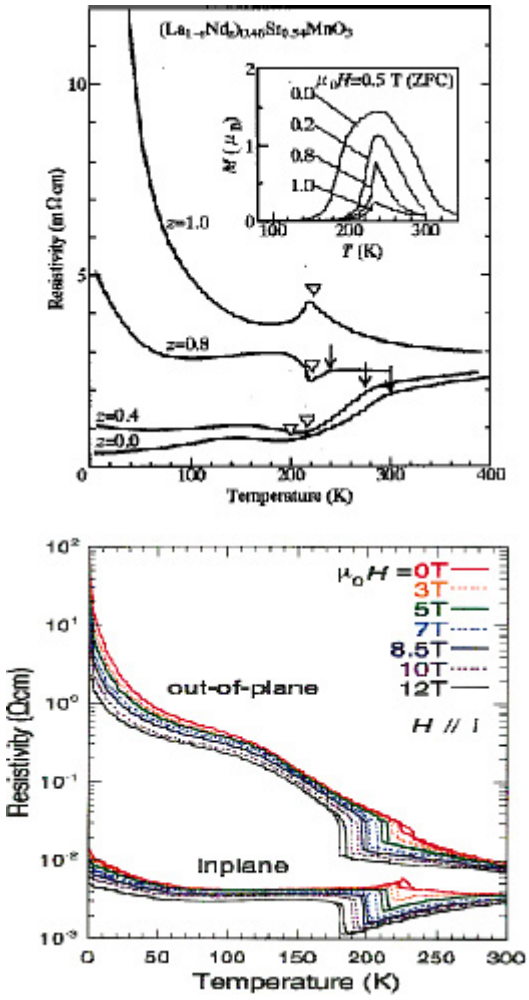

Figure 5. Top: temperature dependence of resistivity of $(La_{1-z}Nd_z)_{1-x}Sr_{0.54}MnO_3$ (after Akimoto *et al* [28]). The arrows and downward triangles denote FM and AFM transition temperatures. The conduction bandwidth decreases with z and a metal–insulator transition occurs. The inset shows magnetization with temperature at four different z values. Bottom: anisotropy between the in-plane and out-of-plane resistivities and the effect of magnetic field on them (reprinted with permission from Kuwahara *et al* [19], copyright (1999) by the American Physical Society). The magnetic field is applied parallel to both current and the respective crystal axes.

resistivity curves in figure 4, lower panel), with a sudden change in the orbital order parameter and lattice parameters. The absence of any superlattice spots in the neutron diffraction [36] across the transition reflects the absence of accompanying CO in either A or C phases.

The electrical resistivity is shown in the lower panel of figure 4. The in-plane resistivity ρ_{ab} is low and metallic (a bad metal) while the out of plane ρ_c is insulating. The large anisotropy of ρ, in spite of a near cubic single crystal system, is an indication of the absence of coherent charge transport and a consequent quenching of the DE mechanism along the c-direction. The situation here can be contrasted with the lightly doped $LaMnO_3$, which also has A-type spin order, and where spin canting in the AF-coupled direction is observed. No canting of spins

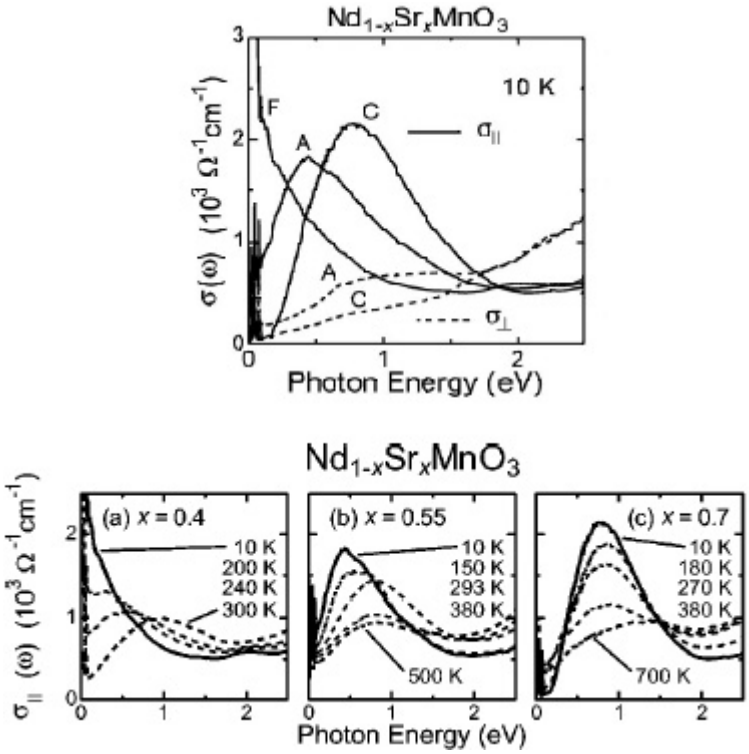

Figure 6. Optical conductivity depends stongly on the polarization shown in three different phases, FM ($x = 0.4$), A type ($x = 0.55$) and C type ($x = 0.7$) in a single crystal of $Nd_{1-x}Sr_xMnO_3$ (reprinted with permission from Tobe *et al* [77], copyright (2004) by the American Physical Society). The lower panel shows the temperature evolution of the spectra.

is observed in the A-type AF phase in the overdoped region and the charge is almost entirely confined in the FM planes.

In the A phase, the effect of magnetic field on resistivity is stronger along the c-direction than in the plane (figure 5). The AF transition temperature decreases with magnetic field as the competing FM state stabilizes. Below T_N, a large negative MR is seen, more prominent in the AF direction. On application of the field normal to the FM planes, there is a tilting of spins out of the plane resulting in an FM component across. This causes the c-axis resistivity to drop considerably, resulting in the large negative MR.

The anisotropy in electronic transport in the orbitally ordered A and C phases is reflected in the optical conductivity as well. Tobe *et al* [77] used a twin-free single crystal and measured the polarization-dependent optical spectra in $R_{1-x}A_xMnO_3$ (where R stands for Pr and Nd, A stands for Sr and Ca) for $x = 0.4, 0.55$ and 0.7. Figure 6 shows the optical conductivity for the electric field (**E**) parallel and perpendicular to the FM direction. The figure clearly shows that (i) $\sigma_{\parallel}(\omega) > \sigma_{\perp}(\omega)$ all the way up to about 1.8 eV and (ii) the Drude weight, present in the FM metallic state at $x = 0.4$, is absent in both the A phase ($x = 0.55$) and the C phase ($x = 0.7$), though in all cases there is a broad tail in $\sigma(\omega)$ persisting up to about 1 eV in the FM state and beyond in A and C phases. The anisotropy between parallel and perpendicular optical conductivity is again a consequence of incoherent charge transport across the orbitally ordered planes (A phase)/chains (C phase).

There is a broad peak in $\sigma_{\parallel}(\omega)$ in mid-spectral range in the A and C phases which Tobe *et al* [77] believe comes from a possible 'pseudogap' (A phase) and a real 'gap' (insulating C phase) in the electronic spectrum. There is no sharp edge in the optical reflectivity or a threshold in $\sigma(\omega)$, and the suggestion for a gap therefore is somewhat tenuous. There is a sudden enhanced absorption at the peak reminiscent of a gap. The angle resolved photoemission spectroscopy [79] shows no indication of a gap in the Fermi surface (FS), although FS nesting is observed [80]. The absence of a Drude peak, the existence of a broad peak at about 0.5–1 eV and the large spectral weight at higher energies certainly indicate the existence of diffuse carrier dynamics and the presence of excitations up to energies about 1.5–2 eV. The temperature dependence (lower panel in figure 6) of $\sigma_{\parallel}(\omega)$ shows a gradual transfer of spectral weight from low energies over to a wide range of energies (>2 eV) [77, 78]. The peak in the mid-spectral range also diminishes gradually with increasing temperature. The integrated $\sigma_{\parallel}(\omega)$, a measure of the effective number of carriers participating in coherent transport, shows a rapid decrease as x changes from 0.4 to 0.55 and 0.7, indicating the suppression of coherent carriers with the dimensionality of the underlying order. The x dependence of the carrier dynamics has been attributed [77] to the formation of short range charge order in the low-dimensional ground states. There are some theoretical predictions [81, 82] of charge ordered states in the A phase that are consistent with the x-dependence of $\sigma_{\parallel}(\omega)$. There is no experimental evidence for the same in the C phase. The diffuse charge dynamics could be due to the strong coupling of the orbital excitations to charge dynamics.

The orbital order in the A phase and the consequent anisotropy in the spin and charge order also shows up in the anisotropy of spin-waves in $Pr_{1-x}Sr_xMnO_3$ [83]. Inelastic neutron scattering at 20 K maps out the spin-wave spectrum in the energy range 2–12 meV and we find that the spin-wave dispersion is much steeper when the neutron momentum transfer **Q** is parallel to the FM planes than when **Q** is normal to it. The Heisenberg model with ferromagnetic exchange along the planes and AF exchange across them [84] and an additional single-ion anisotropy [83] gives a good fit to the experimental spectrum.

2.2. *Effect of disorder*

The doped manganites $R_{1-x}A_xMnO_3$ are intrinsically disordered owing to the substitution of trivalent ions by divalent ones. Although the dopant ions do not enter the active network of MnO_6 octahedra that are considered central to the transport properties and magnetic ordering, their effects cannot be ignored. Indeed, the fairly high resistivities even in the metallic phase are a testimony to the intrinsic disorder present. In this kind of substitution not only are the charges on the dopant ions different from the trivalent rare-earth ions they replace, but also the ionic sizes of the rare earths vary considerably (e.g., La, Nd and Pr all have different ionic sizes). Hence there is a mismatch of ionic sizes between these and the divalent ion (Sr, Ca etc) that replaces them. Such mismatch would quite naturally bring about large lattice distortions as well.

Since the Mn ions are central to the mechanism of magnetic and orbital order in the manganites, substitution at this site would be quite revealing. In the last few years quite a few experimental investigations [68, 69] have been carried out by substitution of Mn by Fe, Ga and Al. These have similar ionic sizes and valences to Mn and therefore cause very little distortion in the lattice [68]. For example, the substitution of Mn^{3+} by Fe^{3+} (which has identical ionic size as Mn^{3+}) in $La_{1-x}Ca_xMn_{1-y}Fe_yO_3$ in the AFM region at $x = 0.53$ shows that the resistivity increases and magnetoresistance disappears by about $y = 0.13$. Although the Fe^{3+} has a higher moment than the Mn^{3+} that it replaces, one observes a steady suppression of the magnetic moment and ferromagnetism with Fe doping [68]. Whether there

is any accompanying change in the underlying magnetic order is not clear. In addition, the systematics across several manganites with different bandwidths are not available yet.

There are two effects when Fe is doped in place of Mn: (i) in the octahedral crystal field the Fe^{3+} (high-spin d^5 configuration) sites have all their $e_{g\uparrow}$ orbitals filled up and forbid the motion of electrons from Mn^{3+} into Fe^{3+} sites preventing the DE mechanism from operating and (ii) the presence of an Fe^{3+} instead of Mn^{3+} in any site alters the superexchange interaction between this and the neighbouring sites.

Although a smaller effect, the depletion of the effective number of electrons taking part in the DE mechanism will reduce the conductivity and move the effective doping x towards the right in the phase diagram and increase AF correlations and resistivity further. There is also the possibility that due to these combined effects the magnetic ground state may get altered, a possibility only further experiments will reveal.

There is another source of scattering coming from the localized t_{2g} spins at each Mn site. The itinerant e_g electrons, in a mean-field sense, can be thought of as moving in a magnetic 'field' of the localized spins because of the Hund's coupling between them. It has been shown [70] that such a random field can indeed localize some of the electronic states, particularly in the low-dimensional bands (as obtains in C and A phases). Substitution of Mn^{3+} by Fe^{3+}, which has a different moment (5/2 as opposed to 2), introduces random changes in this field and additional channels for scattering. The observation [72] of a spin-glass type phase at low temperature in the Cr-doped $La_{0.46}Sr_{0.54}Mn_{1-y}Cr_yO_3$ ($0 < y < 0.08$) is a possible indication of how the competing interactions between the coexisting FM phase in the metallic A-type AFM matrix are affected by scattering off the random magnetic Cr impurity and the resultant localization of mobile charge carriers.

3. Theoretical understanding

3.1. Degenerate DE model

Many of the theoretical efforts in the overdoped regime have been concentrated on the understanding of the complex magnetic and orbital structure observed in the phase diagram. The importance of the degenerate e_g manifold and its relevance in determining the magnetic order have already been emphasized [37, 38, 42]. There have been several detailed theoretical investigations [33, 32, 39–42, 44, 74, 90] to work out the interplay of the orbital and spin order in the overdoped manganites. It is due to these investigations that the role of the orbital degrees of freedom in the magnetic order is now clearly established.

It is primarily the absence of strong JT derived effects (for example the absence of CE phase in most of the manganites at $x = 0.5$ or above) and low Mn^{3+} concentration that render the physics of the region $x > 0.5$ different from that in the $x < 0.5$ for the manganites. In almost all the theoretical descriptions of this region, therefore, the degeneracy of the e_g orbitals is vital. In order to pay due heed to the compelling experimental and theoretical evidence in support of the role of the degenerate e_g orbitals, Brink and Khomskii [37] proposed a model for the electron-doped manganites that incorporates the e_g orbitals and the anisotropic hopping between them. In the undoped $LaMnO_3$ compound each Mn ion is in the Mn^{3+} state and has one electron in the e_g orbital acting as a Jahn–Teller centre. The e_g orbitals are split and the system is orbitally ordered. Thus for the lightly (hole-) doped system one can, at the first approximation, ignore the orbital degree of freedom and apply a single band model like the conventional double exchange (DE) model.

There are $y = 1 - x$ electrons in the two e_g orbitals at each Mn site in the doped manganite $R_{1-x}A_xMnO_3$. The actual filling (electron density), therefore, is $\frac{y}{4}$. This means

that the highest filling in the overdoped region ($0.5 \leqslant x \leqslant 1.0$) is only $\frac{1}{8}$. Because of this low electron concentration and the resulting low number of Jahn–Teller centres, the e_g band is mostly degenerate and the Jahn–Teller effect is negligible to a leading approximation. The neglect of the Jahn–Teller effect is also justified from the experimental evidence presented above [89]. The usual charge and spin dynamics of the conventional DE model then operate here too, though the additional degrees of freedom due to the degenerate set of e_g orbitals make the spin exchange processes more complicated. This model has been referred to as 'double exchange via degenerate orbitals'.

In the limit $x = 1$ the e_g bands are empty and the magnetic order is dominated by the AF superexchange (SE) between t_{2g} spins. As x decreases from unity the band begins to fill up and the KE of electrons in the e_g levels along with the attendant Hund's coupling between the localized and conduction electron spins begins to compete with the AF SE interaction, leading to a rich variety of competing magnetic and orbital structures. The model describing the ground states of the electron-doped manganites is thus

$$H = J_{\mathrm{AF}} \sum_{\langle ij \rangle} \mathbf{S_i} \cdot \mathbf{S_j} - J_{\mathrm{H}} \sum_{i} \mathbf{S_i} \cdot \mathbf{s_i} - \sum_{\langle ij \rangle \sigma,\alpha,\beta} t_{i,j}^{\alpha\beta} c_{i,\alpha,\sigma}^{\dagger} c_{j,\beta,\sigma} \tag{1}$$

$\alpha, \beta = 2(1)$ for $d_{x^2-y^2}(d_{3z^2-r^2})$ orbitals and the hopping matrix elements are determined by the symmetry of e_g orbitals [17, 58]. **S** and **s** denote the localized t_{2g} and itinerant e_g spins respectively. The model is similar to the conventional DE model. Apart from the SE term, the primary difference here is the presence of orbital degeneracy with anisotropic hopping matrix elements $t_{ij}^{\alpha\beta}$ between them. We will argue in the following that this makes its outcome very different [10, 62, 63] from the conventional DE model.

The usual strategy in dealing with manganites is to treat the t_{2g} spins classically [10] and set the Hund's coupling to infinity. In this limit the e_g spins are forced to align along the underlying t_{2g} spins at every site, thereby making the e_g spin degrees irrelevant. The effect of magnetic alignment on hopping can be easily worked out since the core spins are treated classically as vectors with polar angles θ_i and ϕ_i. The electron quantization axis at site i is then rotated to make it parallel to $\mathbf{S}_i$. This is accomplished quite easily by the usual spin-1/2 rotation matrix operating on the two component spinor Ψ_i.

The necessary rotation operator consists of a rotation by θ_i about a new y-axis, obtained from the original one by a rotation of ϕ_i about the z-axis, all rotations positive. The local transformation is then $\exp(\mathrm{i}\frac{\phi_i}{2}\sigma_z)\exp(\mathrm{i}\frac{\theta_i}{2}\sigma_y)\exp(-\mathrm{i}\frac{\phi_i}{2}\sigma_z)$. A similar rotation at site j rotates the electron spin at j. Finally, one reads off the (1, 1) element of the resulting 2×2 matrix in spin space from the transformation of $\Psi_i^{\dagger}\Psi_j$ to get the effective hopping $t_{\mathrm{eff},\langle ij \rangle} = t[\cos\frac{\theta_i}{2}\cos\frac{\theta_j}{2} + \mathrm{e}^{\mathrm{i}(\phi_i-\phi_j)}\sin\frac{\theta_i}{2}\sin\frac{\theta_j}{2}]$.

Canting can then be introduced [37] through the effective hopping matrix elements (neglecting the Berry phase term) $t_{xy} = t\cos(\theta_{xy}/2)$ and $t_z = t\cos(\theta_z/2)$ where $\theta_{xy,z}$ are near-neighbour angles between t_{2g} spins in the xy, z directions. The SE energy per state is simply $E_{\mathrm{SE}} = \frac{J_{\mathrm{AF}}S_0^2}{2}(2\cos\theta_{xy} + \cos\theta_z)$. In this level of approximation, the problem reduces to solving the 2×2 matrix equation $\|t_{\alpha\beta} - \epsilon\delta_{\alpha\beta}\| = 0$ for a system of spinless fermions moving about in two orbitals.

$$\epsilon_{11} = -\tfrac{1}{2}t_{xy}(\cos k_x + \cos k_y) - 2t_z \cos k_z. \tag{2a}$$

$$\epsilon_{12} = \epsilon_{21} = \frac{\sqrt{3}}{2}2t_{xy}(\cos k_x - \cos k_y) \tag{2b}$$

$$\epsilon_{22} = -\tfrac{3}{2}t_{xy}(\cos k_x + \cos k_y). \tag{2c}$$

The hopping matrices $t_{\alpha,\beta}^{x,y,z}$ used here are $t_{\alpha,\beta}^{x} = \begin{pmatrix} -1/4 & \sqrt{3}/4 \\ \sqrt{3}/4 & -3/4 \end{pmatrix}$, $t_{\alpha,\beta}^{y} = -\begin{pmatrix} 1/4 & \sqrt{3}/4 \\ \sqrt{3}/4 & 3/4 \end{pmatrix}$ and $t_{\alpha,\beta}^{z} = -\begin{pmatrix} 1 & 0 \\ 0 & 0 \end{pmatrix}$ in units of the hopping along the z-direction between $d_{3z^2-r^2}$ orbitals.

In the doping region being considered, the deviation from cubic symmetry is very small. The two bands arising from the above Hamiltonian are then filled up to the desired density and the SE energy is added to get the total energy. Minimization of this energy with respect to $\theta_{xy,z}$ gives canting in the plane and across it. Evidently, in the absence of canting (pure phases), the electronic densities of states (DOS) in A and C phases are two and one dimensional respectively. The dispersion introduced by canting has been found to be quite small [74] even for large canting. The sequence of phases follows from the nature of the DOS modulated by the anisotropic overlap of orbitals as well as the DE mechanism. For $x > 0.97$ a canted A-type AFM phase is found from this calculation for all values of $J_{\rm AF}$, whereas in almost all the systems G-type AF phase is observed there. This is also expected on physical grounds as $x \to 1$ is the the limit of an empty e_g band. Similarly, when the AF exchange interaction is close to zero (i.e. the ratio $t/J_{\rm AF} \to \infty$), there should be only a ferromagnetic phase. This is not reproduced at this level of approximation. The difficulty of this orbital-only formulation (i.e., at $J_{\rm H} \to \infty$) is that in this limit the only degree of freedom allowed for the e_g electrons is the KE and the associated canting of t_{2g} spins is therefore considerable. Such a situation is quite unrealistic and an identification of a magnetically ordered state with such large canting is ambiguous at times [74]. In fact, the infinite $J_{\rm H}$ limit is unphysical for the manganites [6, 11, 61]: values for $J_{\rm H}$ reported in various experiments [6, 25], model studies [11, 40, 59] and LDA calculations [61, 64] do not suggest the spin splittings of the e_g band in manganites to be very large. These are typically comparable to (or slightly larger than) the e_g bandwidth. The scale of Coulomb correlations is likely to be even higher [6, 11]. The other consequence of using such large Hund's coupling is that the predictions of low energy excitations (like optical spectra, specific heat, spin fluctuation) are going to be inaccurate. This calculation, though, serves as a useful starting point and the problems are partly resolved [38, 39] when the e_g spin dynamics is allowed into the model and the Hund coupling is taken to be finite. From these studies it was also clear that the JT effect can be ignored, to a first approximation, in this region of doping. This is not the case with bilayer manganites as we show later.

3.2. The limit of finite J_H

In the finite $J_{\rm H}$ limit, the fundamental ingredient is the introduction of the e_g spin degrees of freedom. At finite $J_{\rm H}$, the quantum nature of the transport allows for fluctuations and the e_g spin degrees of freedom, along with anisotropic hopping across the two orbitals, play a central role. In the treatment [38, 39], the uncanted homogeneous ground state with magnetic order is chosen as $\mathbf{S} = \mathbf{S}_0 \exp(\mathrm{i}\mathbf{Q}\cdot\mathbf{r})$, where the choice of $\mathbf{Q}$ determines different spin arrangements for the t_{2g} spins. For canted magnetic structures where the angle between two nearest-neighbour t_{2g} spins is different from that of the pure phases, $\mathbf{S}_i$ is given by $\mathbf{S}_i = S_0(\sin\theta_i, 0, \cos\theta_i)$ with θ_i the local tilt of the core spins from the z-axis and takes all values between 0 and π.

The Hamiltonian, under this approximation, is a matrix involving two spins (up and down), two degenerate orbitals ($d_{x^2-y^2}$ and $d_{3z^2-r^2}$) and two momentum indices ($\mathbf{k}$ and $\mathbf{k}+\mathbf{Q}$).

$$H = \sum_{\mathbf{k},\alpha,\beta,\sigma} \epsilon_{\mathbf{k}}^{\alpha\beta} c_{\mathbf{k}\alpha\sigma}^{\dagger} c_{\mathbf{k}\beta\sigma} - J_{\rm H} S_0 \sum_{\mathbf{k},\alpha} c_{\mathbf{k}\alpha\uparrow}^{\dagger} c_{\mathbf{k}+\mathbf{Q}\alpha\uparrow} + J_{\rm H} S_0 \sum_{\mathbf{k},\alpha} c_{\mathbf{k}\alpha\downarrow}^{\dagger} c_{\mathbf{k}+\mathbf{Q}\alpha\downarrow}. \quad (3)$$

Thus, at finite $J_{\rm H}$ the problem is a 8×8 matrix at each $\mathbf{k}$-point, in contrast to the 2×2 spinless problem for infinite $J_{\rm H}$. The SE part of the energy, in the respective spin configurations, is added as before to the energy obtained from the diagonalization of the above.

The magnetic phase diagram obtained from this [39] was quite similar to the experimental phase diagram of a number of manganites, particularly for the intermediate bandwidth systems such as $Nd_{1-x}Sr_xMnO_3$ and $Pr_{1-x}Sr_xMnO_3$ [29, 35, 27]. It follows the sequence

F → A → C → G for x increasing from 0.5 to 1. There is a small canting along the xy-plane in the G-phase, a precursor to the A phase at lower x, increasing with J_H as expected. The canting reduces with increase in J_{AF}. Canting has also been found in the G–C boundary from a mean-field calculation [33] in the non-interacting degenerate DE model. Inclusion of J–T coupling introduces complicated phase separated regions [33] in the phase diagram. Experimental observations of canting in the overdoped region are rare, though a few [65] observations on $Sm_{1-x}Ca_xMnO_3$ claim that the G phase, for low doping, has small canting.

The A phase was found to have an orbital order of $d_{x^2-y^2}$ type while the C phase is $d_{3z^2-r^2}$ ordered—changing abruptly across the phase boundary as expected. It was revealed [39, 74] that the orbital order is the primary driving force for the DE mechanism in this case and leads to the C- and A-type magnetic orders. The planar $d_{x^2-y^2}$ orbital order in the xy-plane (A phase) and rod-like $d_{3z^2-r^2}$ orbital order in the z-direction (C phase) facilitate hopping of electrons, thereby enhancing the double exchange process. Such a scenario has been borne out in several experiments [28, 35, 45], where evidence for orbital ordering is seen at a higher temperature than the spin ordering. However, in the G and F phases no significant orbital ordering has been observed. Thus the interplay of spin alignment along chains or planes and the corresponding orbital order lead to the transformation from the 1D to the 2D and finally to the 3D magnetic order. The resulting competition between effective KE (determined by J_H, band filling and orbital ordering) and SE leads to the transitions G → C → A → F (the number of AF bonds 6, 4, 2 and 0 per site respectively) with decreasing x.

In most of the intermediate and low bandwidth manganites, a CE-type magnetic order. predicted long ago by Kanamori and Goodenough [16, 3] has been found at $x = \frac{1}{2}$. Using four Q vectors it is possible to define such a magnetic structure in the mean-field analysis. In the non-interacting degenerate DE model, Pai [38] has found this state at $x = 0.5$ at finite J_H. This state is unstable anywhere away from $x = 0.5$ towards A or F phases [74, 74]. The CE phase is also charge ordered (with stacking along the z direction) and orbitally ordered, which were not included in these mean-field calculations. Solovyev and Terakura [90] studied the non-interacting Hamiltonian of equation (1) in the $J_H \to \infty$ limit using a multiple scattering approach. With well defined conventions for different spin orders, they succeeded in recovering the magnetic phases in the x–J_H plane with intermediate regions having significant spin canting. As pointed out by Maezono *et al* [40] and Maitra *et al* [39] earlier, orbital ordering in the A phase forbids KE gain even when there is a finite FM component in the z-direction. No significant canting in either A or C phases (or at their boundaries) has been found by them. It is believed that canting in these regions is primarily an artifact of the infinite J_H approximation and incomplete orbital order. Besides, any finite Coulomb interaction (U') will enhance the orbital order and reduce canting. The possibility of continuous transition between states of different symmetries through canted spin arrangements is greatly reduced in general by pre-emptive first order transitions between them and leads to phase separations [49]. As we discussed earlier, phase segregations are quite common in these systems and have been observed by several groups [12, 32, 34, 90]. There is no definitive experimental evidence for canting in the region of doping where A or C phases are present.

3.3. The interacting model at finite J_H

There is nearly universal agreement [11, 61, 12] that the e_g manifold in manganites is correlated, with the degree of correlation varying across the bandwidth from strong to intermediate. The dominant contributions come from, as usual, the following terms:

$$H_{\text{int}} = U \sum_{i\alpha} \hat{n}_{i\alpha\uparrow}\hat{n}_{i\alpha\downarrow} + U' \sum_{i\sigma\sigma'} \hat{n}_{i1\sigma}\hat{n}_{i2\sigma'} + V \sum_{\langle ij\rangle} \hat{n}_i\hat{n}_j. \tag{4}$$

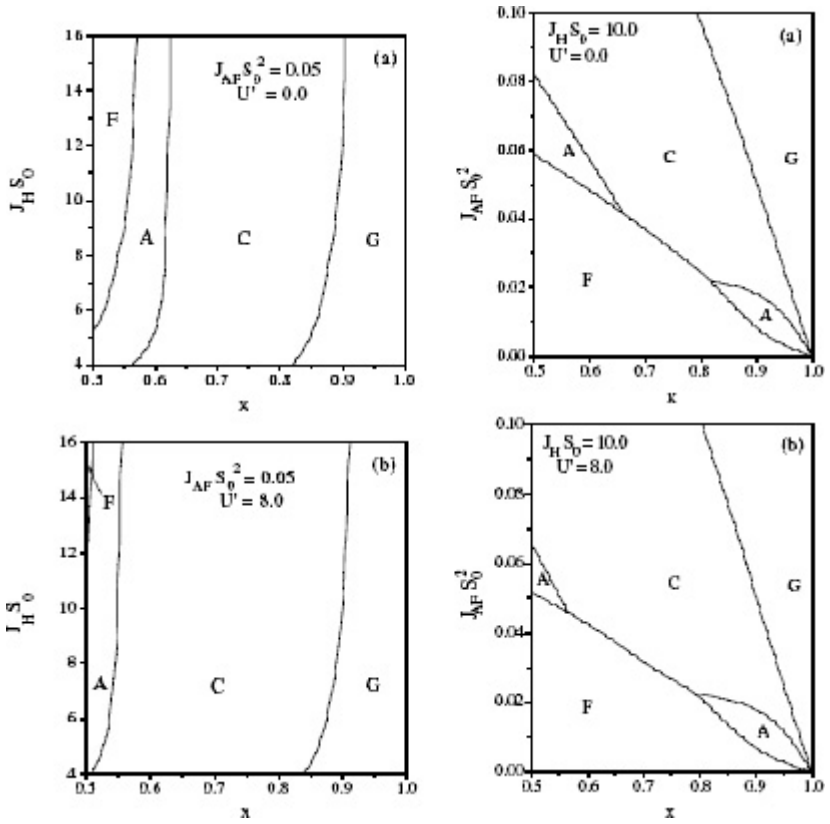

Figure 7. Orbital occupancies are plotted against doping. Orbital order reverses from $d_{x^2-y^2}$ to $d_{3z^2-r^2}$ across the boundary between A- and C-type phases. With increasing U' the orbital order stabilizes.

$\hat{n}_i = \sum_{i\alpha\sigma} \hat{n}_{i\alpha\sigma}$. The U and U' terms are the local intra- and inter-orbital Coulomb interactions. The last term represents the near-neighbour Coulomb repulsion favouring, as it is, a charge ordering in the ground state.

In almost all the theoretical work [39, 40, 74, 74] on the overdoped manganites, the interactions have been treated in the mean-field theory. As pointed out by Hotta *et al* [59], the mean-field theory for the interacting DE model, even in low dimension, gives good agreement with exact diagonalization studies on finite size systems. Comparison of the mean-field phase diagram with exact diagonalization on small systems by Misra *et al* [61] is also encouraging.

The primary effect of U' is to enhance the orbital order, thereby stabilizing the A and C phases. The U term can be neglected for the values of J_H considered. In figure 7 this enhanced orbital order is shown. The A and C phases gain in size slightly, while the F-phase, derived mainly from the KE of the electrons in the e_g band, now shrinks with increasing correlation. These trends are in agreement with the observations of Kajimoto *et al* [29, 35] and Akimoto *et al* [28]. The enhanced correlation acts to reduce the effective KE of the electrons and the progression of the phase diagram follows figures 8(a) and (b) in the two columns and compares well with figure 2, where the effect of e_g bandwidth is depicted.

The Monte Carlo study of Sheng and Ting [66] took the strong correlation point of view in contrast to the band-limit. Projecting out the correlations and the strong JT coupling, they

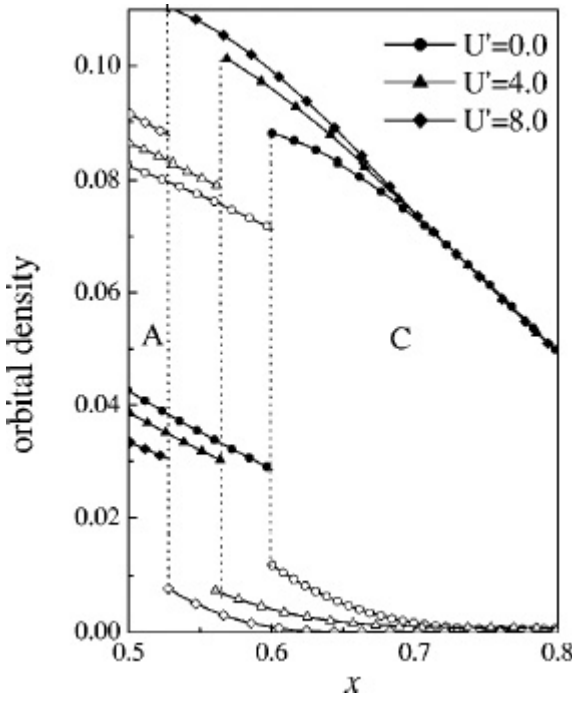

Figure 8. Phase diagram as a function of x with Hund's coupling and SE exchange (left and right columns). The shrinking of FM phase as U' increases is shown in the bottom panel in each column. Inter-orbital correlation increases in each column from (a) to (b).

derive a projected Hamiltonian with an effective hopping dependent on both spin and orbital alignment in neighbouring sites. There is also a spin-orbital coupled term in the effective Hamiltonian. They find a ferromagnetic region at higher temperature close to $x = 0.5$ while at low temperature there are only A and G phases for $x > 0.5$. The ground state in the entire range of doping turns out to be orbitally ordered.

3.4. Charge ordering

The longer range part in equation (4) favours charge ordering (CO) in manganites. The major change observed in the phase diagram is the absence of the A phase and the presence of CO for values of $V > 0.29$. Typical values of V are between 0.2 and 0.5 [6, 11] (in units of t). There are only three phases now—a coexisting ferromagnetic and charge-ordered (F-CO) phase, the orbitally ordered C phase and the G phase. A coexisting F-CO phase close to $x = 0.5$ has been reported by Loudon *et al* [57] from electron microscopy experiments.

The mean-field calculations of Jackeli *et al* [67] with a similar model (with $U = U' = 0$) at $x = 0.5$ also find an F-CO coexistence region at a critical value of $V \approx 0.7$. This value appears to be too high [74] and is possibly an artifact of the infinite J_H limit adopted in their calculations. There is a large body of literature on charge ordering [13, 25, 4] in manganites. There are few model calculations on CO [14] in manganites. Numerical calculations indicate [11] CO states at commensurate filling and a possible CE phase at $x = 0.5$ which has a staggered charge order in the plane.

The anisotropic charge order (or stripes) in the overdoped manganite has not been investigated theoretically so far. Such ground states are indeed a possibility in the regions

where there is an extant orbital order [26]. Whether the JT effect is a necessary requirement for such ground states is still not clear though. In fact, there are claims [85] from a finite temperature mean-field calculation with a degenerate, non-interacting DE model at the infinite J_H limit that without the Jahn–Teller effect the CE phase at $x = 0.5$ in the low bandwidth system is not accessible, though the question is wide open [44] in the presence of Coulomb interactions like U' and V.

As discussed earlier, the manganites have a considerable amount of intrinsic disorder; indeed, phase separation has been seen in many regions of their phase diagram. Electron microscopy reveals a high degree of inhomogeneity and the effects thereof could be extremely important in determining the physical properties [4, 12].

The theoretical models have mainly concentrated on the magnetic and orbital order, and disorder has been completely ignored. To a first approximation, the disorder does not seem to play a major role in the magnetic phase diagram in this region of doping. This is possibly due to the non-magnetic nature of the disorder—the rare earth ions are not found to have any observable moment except for Pr and it has been shown that Pr–Mn coupling does not have a detectable effect [60] in the magnetic structure. There are a few very qualitative attempts to account for the effects of disorder on the magnetic order [74, 86]. There is numerical work on the effect of disorder on the transport properties in manganites and the effects are found to be strong and may even lead to phase separation [87]. It is also not clear what effect the disorder has on the nature of transition across the various phases [54].

3.5. Bilayer manganites

The bilayer manganites had to wait a little longer before attention was paid to them. The phase diagram in the entire range of doping in $La_{2-2x}Sr_{1+2x}Mn_2O_7$ was reported by Ling *et al* [88]. The layered nature of the system prevents coherent transport along the c-direction and therefore the FM phase is absent in the region $x > 0.5$. The successive phases are A $\rightarrow$ C $\rightarrow$ G with increasing x. In the range $0.66 < x < 0.74$ a region without apparent long range order is also observed. Beyond this the AF C-type order (and a polytype, C′ phase, where the spins are aligned along the basal plane b-axis) is found. For $x > 0.90$ a G-phase region is observed, with a possible CG coexistence region in between. The phase diagram and the spin orders observed are shown in figure 9 after Ling *et al* [88].

The layered nature of the underlying structure in $La_{2-2x}Sr_{1+2x}Mn_2O_7$ is expected to favour an A-type spin arrangement. Even the CE phase, present in most of the 3D manganites at $x = 0.5$, is replaced by the layered A-type order in $La_{2-2x}Sr_{1+2x}Mn_2O_7$ at the same filling (with possibly a charge-ordered state [92, 93] coexisting $x = 0.5$). Model calculations [38, 94] also show only A-type instability in the overdoped bilayer systems.

There is a tetragonal–orthorhombic distortion associated with the elongation along the basal b-axis [88] near $x = 0.74$ (figure 9) where the C phase first appears. There is no buckling of the octahedron across the transition. It is this static distortion, acting like a 'field' in the orbital space through local electrostatic coupling, that orients the orbitals in a suitable arrangement and leads to the C (or C′) phase [75]. In a low dimensional system, the effect of structural distortion, at such low filling, is expected to be considerable. Any model, therefore, should include this coupling. A mean-field calculation in the same manner as for the 3D manganites, including this lattice coupling to orbitals, $H_{el} = g\sum_{i,n}\tau_{i,n}Q_{i,n}$, does indeed reproduce the correct phase diagram [75]. $Q_{i,n}(n = 1, 2)$ are the even-parity local distortions of an MnO_6 octahedron and $\tau_{1,2}$ represent the first and third Pauli matrices. It is again the preferred orbital orders in the A and C/C′ phases that give rise to the magnetic order. The phase diagram is reproduced in figure 10 (after Maitra *et al* [75]). The region close to

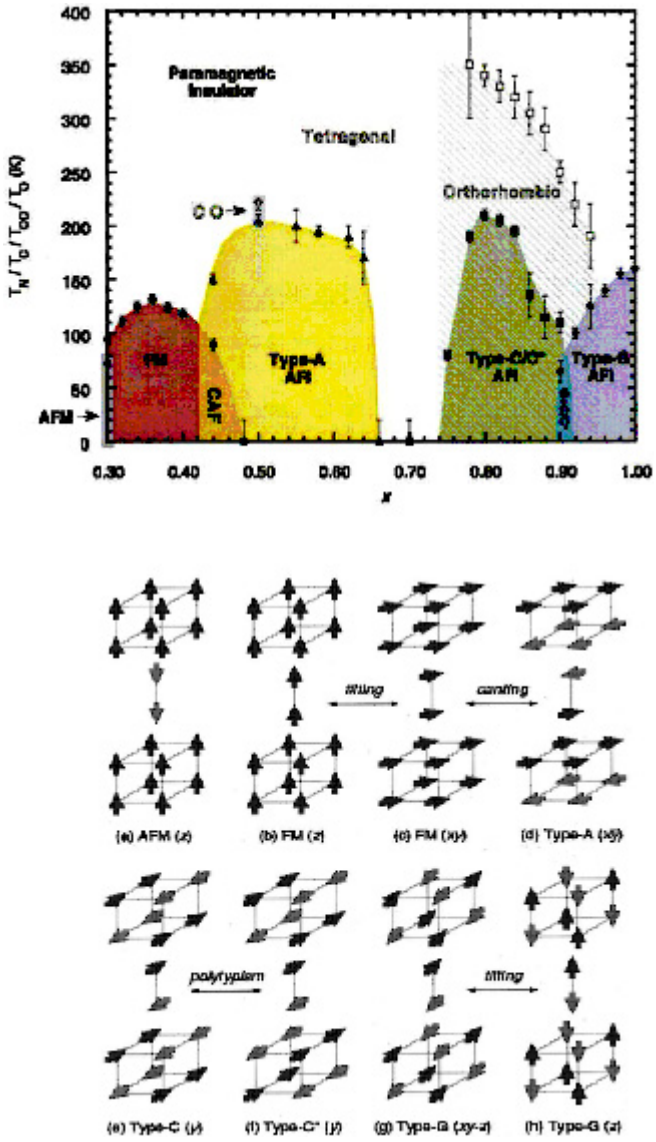

Figure 9. The upper panel shows the phase diagram of bilayer manganites while the lower panel shows the underlying magnetic structures (reprinted with permission from Ling *et al* [88], copyright (2000) by the American Physical Society).

$x = 0.5$ is layered antiferromagnetic with a coexisting charge order [92, 93]. Inclusion of a near-neighbour repulsion term in the above model shows such a coexistence region [76].

4. Conclusion

The overdoped manganites have physical properties that bear close resemblance to the underdoped side in many respects, although there are crucial differences. These differences, as discussed above, owe their origin primarily to the rarity of Jahn–Teller sites, leading to

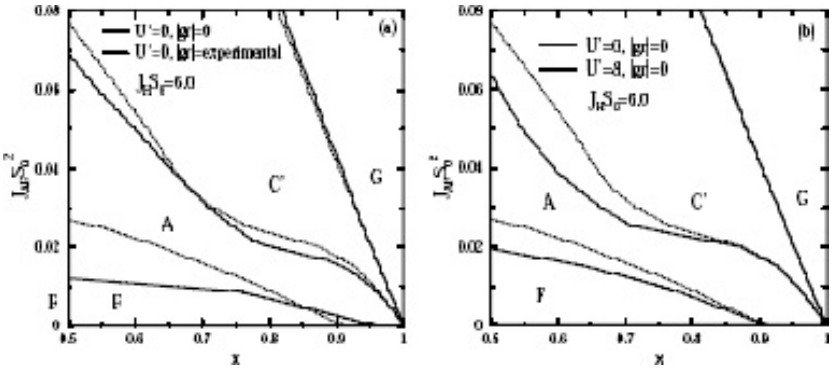

Figure 10. Phase diagram of bilayer manganites showing the effects of both lattice distortion and U' (after Maitra *et al* [75]).

an effectively degenerate set of e_g orbitals in the overdoped region. The orbital order, being probably of secondary importance in the underdoped side, plays a major role in facilitating the magnetic and magnetotransport behaviour in the overdoped regime. The optical spectra clearly show a broad range of excitations at energies around 1 eV and beyond, coming from the orbital fluctuations and the attendant cooperative structural relaxations. Theoretical models have been quite successful in predicting the ground states of both three dimensional and bilayer manganites. The strong coupling of charge, spin and orbital degrees and the lack of separation in energy scales between these couplings have made calculations of the excitations fairly complicated. In the near future, a lot more experiments are expected to address the issues that are unresolved as yet. The idea of strongly coupled charge, orbital and lattice degrees of freedom is quite fascinating. In the overdoped regime, it appears that the JT effects could be ignored in the first approximation, but a more microscopic justification of this has not yet arrived.

Acknowledgments

The author acknowledges collaboration with Tulika Maitra and Hans Beck on several issues discussed here. The hospitality extended by the Max Planck Institute for the Physics of Complex Systems in Dresden, where a part of the article was written, is gratefully acknowledged.

References

[1] Jonker G H and van Santen J H 1950 *Physica* **16** 337
Jonker G H and van Santen J H 1950 *Physica* **16** 599
[2] Wollan E O and Koehler W C 1955 *Phys. Rev.* **100** 545
[3] Goodenough J B 1955 *Phys. Rev.* **100** 564
[4] Tokura Y 2000 *Colossal Magnetoresistive Oxides* (London: Gordon and Breach)
[5] Kaplan T A and Mahanty S D (ed) 1999 *Physics of Manganites* (New York: Kluwer–Academic)
[6] Coey J M D, Viret M and von Molnar S 1999 *Adv. Phys.* **48** 167
[7] Salamon M B and Jaime M 2001 *Rev. Mod. Phys.* **73** 583
[8] von Helmholtz R, Wecker J, Holzapfel B, Schultz L and Samwer K 1993 *Phys. Rev. Lett.* **71** 2331
[9] Jin S *et al* 1994 *Science* **264** 413
[10] Zener C 1951 *Phys. Rev.* **82** 403
Anderson P W and Hasegawa H 1955 *Phys. Rev.* **100** 675

[11] Dagotto E, Hotta T and Moreo A 2001 *Phys. Rep.* **344** 1
[12] Dagotto E 2003 *Nanoscale Phase Separation and Colossal Magnetoresistance* (Berlin: Springer)
[13] Pandit R and Taraphder A 2006 unpublished
[14] Cepas O, Krishnamurthy H R and Ramakrishnan T V 2006 *Phys. Rev.* B **73** 035218
[15] Kanamori K 1960 *J. Appl. Phys.* Suppl. to **31** 14S
[16] Kanamori K 1959 *J. Phys. Chem. Solids* **10** 87
[17] Kugel K and Khomskii D I 1972 *JETP Lett.* **15** 446
Kugel K and Khomskii D 1973 *Sov. Phys.—JETP* **37** 725
[18] Kuwahara H, Tomioka Y, Asamitsu A, Moritomo Y and Tokura Y 1995 *Science* **270** 961
[19] Kuwahara H, Okuda T, Tomioka Y, Asamitsu A and Tokura Y 1999 *Phys. Rev. Lett.* **82** 4316
[20] Kuwahara H *et al* 1997 *Phys. Rev.* B **56** 9386
[21] Tomioka Y, Asamitsu A, Moritomo Y, Kuwahara H and Tokura Y 1995 *Phys. Rev. Lett.* **74** 5108
[22] Hejtmanek J, Pollert E, Jirák Z, Sedmidubsk D, Strejc A, Maignan A, Martin Ch, Hardy V, Kuzel R and Tomioka Y 2002 *Phys. Rev.* B **66** 014426
[23] Tomioka Y, Tomioka Y, Asamitsu A, Kuwahara H, Moritomo Y and Tokura Y 1996 *Phys. Rev.* B **53** R1689
[24] Urushibara A, Moritomo Y, Arima T, Asamitsu A, Kido G and Tokura Y 1995 *Phys. Rev.* B **51** 14103
[25] Imada M, Fujimori A and Tokura Y 1998 *Rev. Mod. Phys.* **70** 1039
[26] Oles A M, Cuoco M and Perkins N B 2000 *Lectures on the Physics of Highly Correlated Electron Systems IV* (*AIP Conf. Proc.* vol 527) ed F Mancini (New York: AIP) (*Preprint* cond-mat/0012013)
[27] Hejtmanek J, Jirak Z, Pollert E, Sedmidubsky D, Strec A, Martin C, Maignan A and Hardy V 2002 *J. Appl. Phys.* **91** 8275
[28] Akimoto T, Maruyama Y, Moritomo Y, Nakamura A, Hirota K, Ohoyama K and Ohashi M 1998 *Phys. Rev.* B **57** R5594
[29] Kajimoto R, Yoshizawa H, Tomioka Y and Tokura Y 2002 *Phys. Rev.* B **66** 180402(R) (*Preprint* cond-mat/0110170)
[30] Jirac Z, Krupika S, Nekvasil V, Pollert E, Villeneuve G and Zounová F 1980 *J. Magn. Magn. Mater.* **15–18** 519
Jirac Z, Krupika S, imaM Dlouhá Z and Vratislav S 1985 *J. Magn. Magn. Mater.* **53** 153
[31] Kawano H, Kajimoto R, Yoshizawa H, Tomioka Y, Kuwahara H and Tokura Y 1997 *Phys. Rev. Lett.* **78** 4253
[32] Ishihara S, Inoue I and Maekawa S 1996 *Physica* C **263** 130
Ishihara S, Inoue I and Maekawa S 1997 *Phys. Rev.* B **55** 8280
[33] Ohsawa T and Inoue J 2002 *Phys. Rev.* B **65** 134442
[34] Machida A *et al* 2002 *J. Phys. Soc. Japan* **71** 27
[35] Kajimoto R, Yoshizawa H, Kawano H, Kuwahara H, Tokura Y, Ohoyama K and Ohash M 1999 *Phys. Rev.* B **60** 9506
[36] Yoshizawa H, Kawano H, Fernandez-Baca J A, Kuwahara H and Tokura Y 1998 *Phys. Rev.* B **58** R571
[37] van den Brink J and Khomskii D 1999 *Phys. Rev. Lett.* **82** 1016
[38] Venkateswara Pai G 2001 *Phys. Rev.* B **63** 064431
[39] Maitra T and Taraphder A 2002 *Europhys. Lett.* **59** 896
[40] Maezono R, Ishihara S and Nagaosa N 1998 *Phys. Rev.* B **57** R13993
[41] Maezono R, Ishihara S and Nagaosa N 1998 *Phys. Rev.* B **58** 11583
[42] Khomskii D and Sawatzky G A 1997 *Solid State Commun.* **102** 87
[43] Hayashi T *et al* 2001 *Phys. Rev.* B **65** 024408
[44] van den Brink J, Khaliullin G and Khomskii D 1999 *Phys. Rev. Lett.* **83** 5118
van den Brink J, Khaliullin G and Khomskii D 2002 *Preprint* cond-mat/0206053
[45] Zimmermann M V, Hill J P, Gibbs D, Blume M, Casa D, Keimer B, Murakami Y, Tomioka Y and Tokura Y 1999 *Phys. Rev. Lett.* **83** 4872
[46] Moreo A, Yunoki S and Dagotto E 1999 *Science* **283** 2034
[47] Uehara M, Mori S, Chen C H and Cheong S-W 1999 *Nature* **399** 560
Podzorov V, Uehara M, Greshenson M E, Koo T Y and Cheong S-W 2000 *Phys. Rev.* B **61** R3784
[48] Rao C N R and Raveau B (ed) 1998 *Colossal Magnetoresiatance, Charge Ordering and Related Properties of Manganese Oxides* (Singapore: World Scientific)
[49] Nagaev E L 1979 *Physics of Magnetic Semiconductors* (Moscow: Mir)
Nagaev E L 1970 *Sov. Phys.—JETP* **30** 693
Nagaev E L 1997 *Physica* B **230–232** 816
Nagaev E L 1996 *Phys.—Usp.* **39** 781
[50] Yu Kagan M, Khomskii D I and Mostovoy M V 1999 *Eur. Phys. J.* B **12** 217
Yu Kagan M, Kugel K I and Khomskii D I 2001 *J. Exp. Theor. Phys.* **93** 415
[51] Guinea F, Gomez-Santos G and Arovas D P 2000 *Phys. Rev.* B **62** 391

[52] Alonso J L, Ferdinandez L A, Guinea F, Laliena V and Martin-Mayor V 2000 *Phys. Rev.* B **63** 64416
[53] Dagotto E, Burgy J and Moreo A 2002 *Preprint* cond-mat/0209689 and references therein
[54] Burgy J, Mayr A, Martin-Mayor V, Moreo A and Dagotto E 2001 *Phys. Rev. Lett.* **87** 277202
[55] Renner Ch, Aeppli G, Kim B-G, Soh Y-Ah and Cheong S-W 2002 *Nature* **416** 518
[56] Yunoki S, Hu J, Malvezzi A L, Moreo A, Furukawa N and Dagotto E 1998 *Phys. Rev. Lett.* **80** 845
Yunoki S, Moreo A and Dagotto E 1998 *Phys. Rev. Lett.* **81** 5612
[57] Loudon J C, Mathur N D and Midgley P A 2002 *Nature* **420** 797
[58] Slater J C and Koster G F 1954 *Phys. Rev.* **94** 1498
[59] Hotta T, Malvezzi A and Dagotto E 2000 *Phys. Rev.* B **62** 9432
[60] Hwang H Y, Dai P, Cheong S-W, Aeppli G, Tennant D A and Mook H A 1998 *Phys. Rev. Lett.* **80** 1316
[61] Misra S, Pandit R and Satpathy S 1997 *Phys. Rev.* B **56** 2316
Misra S, Pandit R and Satpathy S 1999 *J. Phys.: Condens. Matter* **11** 8561
[62] Furukawa N 1995 *J. Phys. Soc. Japan* **67** 2734
Furukawa N 1999 *Physics of Manganites* ed T A Kaplan and S D Mahanty (New York: Kluwer–Academic) and references therein
[63] Kubo K and Ohata N 1972 *J. Phys. Soc. Japan* **33** 21
[64] Satpathy S, Popovic Z S and Vukajlovic F R 1996 *Phys. Rev. Lett.* **76** 960
[65] Maignan A, Martin C, Damay F and Raveau B 1998 *Phys. Rev.* B **58** 2758
Mahendiran R, Maignan A, Martin C, Hervieu M and Raveau B 2000 *Phys. Rev.* B **62** 11644 It is not clear though if there is phase separation between different magnetic phases in these regions rather than canting
[66] Sheng L and Ting C S 1998 *Preprint* cond-mat/9812374
[67] Jackeli G, Perkins N B and Plakida N M 2001 *Phys. Rev.* B **62** 372
[68] Ahn K H, Wu X W, Liu K and Chien C L 1997 *J. Appl. Phys.* **81** 5505
[69] Blasco J, García J, de Teresa J M, Ibarra M R, Perez J, Algarabel P A, Marquina C and Ritter C 1997 *Phys. Rev.* B **55** 8905
[70] Cerovsky V, Mahanti S D, Kaplan T A and Taraphder A 1999 *Phys. Rev.* B **59** 13977
[71] Jirac Z, Hejtmanek J, Knizek K, Marysko M, Martin C, Maignan A and Hervieu M 2002 *Preprint* cond-mat/0212517
[72] Dho J, Kim W S and Hur N H 2002 *Phys. Rev. Lett.* **89** 027202
[73] Maezono R, Ishihara S and Nagaosa N 1998 *Phys. Rev.* B **57** R13993
Maezono R, Ishihara S and Nagaosa N 1998 *Phys. Rev.* B **58** 11583
[74] Maitra T and Taraphder A 2002 *Phys. Rev.* B **68** 174416
[75] Maitra T and Taraphder A 2004 *Europhys. Lett.* **65** 262
[76] Maitra T, Taraphder A and Beck H 2005 *J. Phys.: Condens. Matter* **17** 4333
[77] Tobe K *et al* 2004 *Phys. Rev.* B **69** 014407
[78] Tobe K *et al* 2003 *Phys. Rev.* B **67** 140402(R)
[79] Chuang Y-D *et al* 2001 *Science* **292** 1509
[80] Campbell B J *et al* 2002 *Phys. Rev.* B **65** 014427
[81] Mizokawa T and Fujimori A 1997 *Phys. Rev.* B **56** R493
[82] Mack F and Horsch P 1999 *Phys. Rev. Lett.* **82** 3160
[83] Krishnamurthy V V *et al* 2006 *Phys. Rev.* B **73** 060404(R)
[84] Raczkowski M and Oles A M 2002 *Phys. Rev.* B **66** 094431
[85] Yu U, Jo Y and Min B I 2002 *Preprint* cond-mat/0209230
[86] Alonso J L, Fernandez L A, Guinea F, Laliena V and Martin-Mayor V 2001 *Preprint* cond-mat/0111244
[87] Kumar S and Majumdar P 2004 *Phys. Rev. Lett.* **92** 126602
[88] Ling C D, Millburn J E, Mitchell J F, Argyriou D N, Linton J and Bordallo H N 2000 *Phys. Rev.* B **62** 15096
[89] Ramakrishnan T V, Krishnamurthy H R, Hassan M and Pai G V 2004 *Phys. Rev. Lett.* **92** 157203 appear to justify quantitatively the ineffectiveness of J–T physics for large x
[90] Solovyev I V and Terakura K 2001 *Phys. Rev.* B **63** 174425
[91] The complicated orbital order of this phase is beyond the homogeneous mean-field approach used. So this spin order can hardly be called the conventional CEphase. The $(\pi, \pi, 0)$ CO associated with the CEphase was not obtainable from the long-range interaction used here.
[92] Kubota M *et al* 1999 *J. Phys. Chem. Solids* **60** (*Preprint* cond-mat/9902288)
[93] Coldea A *et al* 2002 *Phys. Rev. Lett.* **89** 277601
[94] Maezono R and Nagaosa N 2000 *Phys. Rev.* B **61** 1189